NASA TM X-204

[redacted]

[redacted]

TECHNICAL MEMORANDUM
X-204

HIGH SUBSONIC INVESTIGATION OF THE AERODYNAMIC CHARACTERISTICS OF A HYPERSONIC GLIDER MODEL WITH AND WITHOUT DEFLECTED ELEVONS AND BODY FLAP

By F. E. West, Jr., Charles D. Trescot, Jr., and Alfred N. Wiley, Jr.

Langley Research Center
Langley Field, Va.

[redacted]

[redacted]

NATIONAL AERONAUTICS AND SPACE ADMINISTRATION
WASHINGTON February 1960

[redacted]

NATIONAL AERONAUTICS AND SPACE ADMINISTRATION

TECHNICAL MEMORANDUM X-204

HIGH SUBSONIC INVESTIGATION OF THE AERODYNAMIC CHARACTERISTICS OF A HYPERSONIC GLIDER MODEL WITH AND WITHOUT DEFLECTED ELEVONS AND BODY FLAP*

L745

By F. E. West, Jr., Charles D. Trescot, Jr.
and Alfred N. Wiley, Jr.

SUMMARY

A wind-tunnel investigation has been made to study the effects of symmetrical elevon deflection, body flap deflection, and wing plan-form and vertical-tail modifications on the aerodynamic characteristics of a hypersonic glider model at a Mach number of about 0.94. Results were also obtained for the basic model at Mach numbers of 0.60 and 0.78. The model had a 70° swept low wing and upper surface wing-tip vertical tails. Elevon deflection was varied from -30.8° to 15.5°; body flap deflection, from 0° to 30.6°; angle of attack, from about -5° to 14°; and angle of sideslip was also varied for some configurations.

The results show that changing the Mach number from 0.60 to 0.92 had only small effects on the model longitudinal aerodynamic characteristics. The elevons provided adequate trim for the range of angles of attack investigated. Canting the vertical tails outward 30° caused increases in normal force and more negative pitching moments at positive normal-force coefficients. With the tails on, the model had approximately neutral directional stability and generally positive effective dihedral.

INTRODUCTION

Investigations have been initiated in various Langley wind-tunnel facilities to provide information from landing to hypersonic speeds on the aerodynamic characteristics of several hypersonic glider models.

[redacted]

This paper presents the high subsonic static aerodynamic results which were obtained on one of these configurations with and without modifications. The basic model has a 70° swept low wing with wing-tip vertical tails. The results show the effects of symmetrical elevon deflection, body flap deflection, and wing plan-form and vertical-tail modifications on the model aerodynamic characteristics at a Mach number of about 0.94. Results are also shown for the basic model at Mach numbers of 0.60 and 0.78. Five-component balance data (no drag data) were obtained at angles of attack of about -5° to 14°. Some configurations were also tested at angles of sideslip. High subsonic results for other hypersonic glider configurations are presented in references 1 to 3.

L
7
4
5

SYMBOLS

The forces and moments are referenced to the body axes which have their origin on the plane of symmetry at 57.2 percent of the body length and 11.2 percent of the wing span above the wing lower surfaces.

A aspect ratio

b wing span

C_N normal-force coefficient, $\frac{\text{Normal force}}{q_\infty S}$

C_Y side-force coefficient, $\frac{\text{Side force}}{q_\infty S}$

$C_{Y_\beta} = \frac{\partial C_Y}{\partial \beta}$ per degree

C_l rolling-moment coefficient, $\frac{\text{Rolling moment}}{q_\infty Sb}$

$C_{l_\beta} = \frac{\partial C_l}{\partial \beta}$ per degree

C_m pitching-moment coefficient, $\frac{\text{Pitching moment}}{q_\infty S\bar{c}}$

C_n yawing-moment coefficient, $\frac{\text{Yawing moment}}{q_\infty Sb}$

[redacted]

$C_{n_\beta} = \frac{\partial C_n}{\partial \beta}$ per degree

$\bar{c}$ wing mean aerodynamic chord

M_∞ free-stream Mach number

q_∞ free-stream dynamic pressure

L-745

r radius

S total wing area

α angle of attack

β angle of sideslip

δ_f body flap deflection, positive when trailing edge is down

δ_e elevon deflection, positive when trailing edge is down

Model designations:

B_7 fuselage

F_4 body flap

V_9 vertical tails with span in Z-plane

V_{9_A} vertical tails with span tilted outward 30° from the Z-plane

W_7 basic wing

W_{7_A} wing with short chord

MODELS AND APPARATUS

Sketches and dimensions of the basic model with the body flap designated $B_7F_4W_7V_9$ and other model configurations are presented in figure 1. A photograph of the basic model is shown in figure 2. The wing W_7 of the basic configuration had a 70° swept leading edge, an aspect ratio of 1.03, and a taper ratio of 0.27. It was equipped with plain flap-type elevons and each elevon had an area of 0.5 square inch. The alternate wing W_{7_A}, which was similar to wing W_7 except for a modification in the trailing-edge region, had an aspect ratio of 1.11 and a taper ratio of 0.29. Wing-tip vertical tails, designated as V_9, were attached normal to the wing lower surfaces on both wings. The vertical tails designated as V_{9_A}, which were also used on wing W_7, were canted 30° outward with respect to the model plane of symmetry. In some cases a body flap F_4 was deflected on configuration $B_7W_7V_9$. Without the vertical tails on the model, the wing semispan was reduced from 1.789 inches to 1.734 inches. For the W_7 and W_{7_A} wings the balance center is located at 40 and 43.3 percent of the wing mean aerodynamic chord, respectively. All model components are made of steel.

L
7
4
5

The model was mounted on an internal 5-component electrical strain-gage balance that was attached to the sting-support system in the Langley transonic blowdown tunnel. This tunnel which has an octagonal slotted throat section measures 26 inches between flats.

TESTS

Normal-force, pitching-moment, rolling-moment, yawing-moment, and side-force balance data were obtained for the various configurations. All configurations were tested through an angle-of-attack range of about -5° to 14° at an angle of sideslip of approximately 0°. Configurations $B_7W_7V_9$, $B_7W_{7_A}V_9$, and B_7W_7 were also tested through the angle-of-attack range at an angle of sideslip of about 5°. In addition, configuration $B_7W_7V_9$ was tested at angles of sideslip of about -1° to 8° for an angle of attack of about 0°. The basic model $B_7W_7V_9$ was tested at Mach numbers of 0.60, 0.78, and 0.92. The other configurations were tested only at a Mach number of about 0.92.

Model $B_7W_7V_9$ was tested with elevons symmetrically deflected at -30.8°, -15.2°, 0°, and 15.5°. It was also investigated with the lower surface body flap $\left(\text{configuration } B_7F_4W_7V_9\right)$ at 0°, 15.5°, and 30.6°.

Transition strips consisting of 0.001- to 0.002-inch carborundum grains spread on a thin wet coating of shellac were applied to the model surfaces. The grain size selected was approximately the minimum size to cause boundary-layer transition according to the results of reference 4. The strips were 1/16 of an inch in width and the grains covered 5 to 10 percent of the strip area. These strips were put on the upper and lower surfaces of the wing, the side surfaces of the tails, and on the body nose. Leading edges of the strips were located at 5 percent of the wing chord, 7.5 percent of the vertical-tail chord, and at the periphery of the body nose.

Average Reynolds numbers, based on the mean aerodynamic chord, were 2.48×10^6, 2.52×10^6, and 2.54×10^6 at Mach numbers of 0.60, 0.78, and 0.92, respectively, for the configurations having the W_7 wing. For model $B_7W_{7_A}V_9$ the average Reynolds number was 2.35×10^6 at a Mach number of 0.92.

L745

PRECISION

Estimated accuracy of the coefficients (based on balance accuracy) and of other pertinent parameters are indicated below:

C_N	±0.01
C_m	±0.002
C_l	±0.002
C_n	±0.001
C_Y	±0.005
α, deg	±0.1
β, deg	±0.1
M_∞	±0.025

No corrections due to tunnel wall effects or sting interference have been applied to the data. It is believed that these corrections would be small. (See refs. 5 and 6.)

RESULTS AND DISCUSSION

Longitudinal Aerodynamic Characteristics

The effects of Mach number on the longitudinal aerodynamic characteristics of model $B_7W_7V_9$ are presented in figure 3. Summary curves showing the effect of Mach number on the variation of longitudinal center-of-pressure location and longitudinal stability parameter with normal-force coefficient for this model are presented in figure 4. Both of these figures show that the effects of Mach number were generally small.

Figures 5 and 6 show the effect of elevon and body flap deflection, respectively, on the longitudinal aerodynamic characteristics of model

$B_7W_7V_9$ at a Mach number of about 0.93. The results of figure 5 show that the elevons can provide adequate trim for the range of angles of attack investigated. Elevon deflection usually had only minor effects on the shape of the normal-force and pitching-moment curves. Figure 6 shows that deflection of the body flaps generally decreased the normal-force coefficient and made the pitching-moment coefficients less negative. Apparently, the separated region which caused reduced pressures on the lower wing surface behind the flap had a larger effect on normal force than the increased pressures occurring on the flap and on the lower wing surface ahead of the flap. With regard to pitching moment, however, the long moment arm of the increased pressure region with respect to the model moment center probably was the predominant cause of the less negative pitching-moment coefficients.

L
7
4
5

A comparison of the longitudinal aerodynamic characteristics of models $B_7W_7V_9$ and $B_7W_{7_A}V_9$ is presented in figure 7 for a Mach number of 0.92. The relatively small differences between the W_7 and W_{7_A} wings had only small effects on the normal-force and pitching-moment coefficients. The higher normal-force coefficients for the model with the W_{7_A} wing can probably be attributed to the slightly higher aspect ratio for this model.

Figure 8 shows the effect of tail configuration on the longitudinal aerodynamic characteristics for model B_7W_7 at an average Mach number of about 0.94. Without the tails on the model, the normal-force curve was nonlinear. The increase in slope at moderate angles of attack is typical for low-aspect-ratio wings at both subsonic and transonic speeds (for example, see ref. 7) and is associated with viscous effects on the wing upper surfaces. Reference 8 presents a method for estimating this nonlinear effect and a comparison of this method with experimental results for two hypersonic glider models is presented in reference 1. Adding the tails to the model (see fig. 8) increased the normal-force curve slope at low angles and caused the curves to become more nearly linear over most of the angle-of-attack range. These changes are associated with the end-plate effects of the vertical tails; that is, the tails increased the effective aspect ratio of the model. Canting the vertical tails outward 30° increased the normal-force coefficients, as would be expected. It also caused more negative pitching-moment coefficients at positive normal-force coefficients since the increases in normal force occurred behind the origin of the body axes.

Lateral Aerodynamic Characteristics

The effects of tail configuration on the lateral stability derivatives (determined from tests at angles of sideslip of 0° and about 5°) of model B_7W_7 at an average Mach number of about 0.95 are shown in figure 9. Adding either of the tail configurations to the model caused a change in directional stability from unstable to generally neutral. Although the tail-off configuration had positive effective dihedral above an angle of attack of 1°, adding the V_9 tails extended this range at the lower angles. Adding the V_{9_A} tails provided positive effective dihedral throughout the angle-of-attack range.

L
7
4
5

Figure 10 shows the effect of angle of sideslip on the lateral aerodynamic characteristics of model $B_7W_7V_9$ at an angle of attack of 0° and a Mach number of 0.94. This configuration generally had directional stability and positive effective dihedral throughout the angle-of-sideslip range of approximately -2° to 8°.

CONCLUSIONS

A wind-tunnel investigation has been made to study the effect of symmetrical elevon deflection, body flap deflection, and wing plan-form and vertical-tail modifications on the aerodynamic characteristics of a hypersonic glider model at a Mach number of about 0.94. Results were also obtained for the basic model at Mach numbers of 0.60 and 0.78. The basic model had a 70° swept low wing and upper surface wing-tip vertical tails. Elevon deflection was varied from -30.8° to 15.5° and body flap deflection was varied from 0° to 30.6°. Results which were obtained at angles of attack from about -5° to 14° and at angles of sideslip for some configurations indicate the following:

1. The effects on the longitudinal aerodynamic characteristics of the model of changing Mach number from 0.60 to 0.92 were small.

2. The elevons provided adequate trim for the range of angles of attack investigated.

3. Canting the vertical tails outward 30° caused increases in normal force and more negative pitching moments at positive normal-force coefficients.

4. With the tails on, the model had approximately neutral directional stability and generally positive effective dihedral.

Langley Research Center,
National Aeronautics and Space Administration,
Langley Field, Va., September 8, 1959.

L
7
4
5

REFERENCES

1. West, F. E., Jr., Trescot, Charles D., Jr., and Wiley, Alfred N., Jr.: Aerodynamic Characteristics for Two Hypersonic Glider Models With and Without Wing and Vertical-Tail Trailing-Edge Chord-Extensions at a Mach Number of 0.94. NASA TM X-66, 1959.

2. West, F. E., Jr., Trescot, Charles D., Jr., and Wiley, Alfred N., Jr.:
Effect of Vertical Tail and Rudder Deflection on the Aerodynamic
L Characteristics of a Hypersonic Glider Model at Mach Numbers of
7 About 0.62 and 0.93. NASA TM X-189, 1959.
4
5 3. Trescot, Charles D., Jr., West, F. E., Jr., and Wiley, Alfred N , Jr.:
Effects of Elevon Deflection on the Aerodynamic Characteristics of a Hypersonic Glider Model at Mach Numbers of About 0.62 and 0.96. NASA TM X-203, 1959.

4. Braslow, Albert L., and Knox, Eugene C.: Simplified Method for Determination of Critical Height of Distributed Roughness Particles for Boundary-Layer Transition at Mach Numbers From 0 to 5. NACA TN 4363, 1958.

5. Whitcomb, Charles F., and Osborne, Robert S.: An Experimental Investigation of Boundary Interference on Force and Moment Characteristics of Lifting Models in the Langley 16- and 8-Foot Transonic Tunnels. NACA RM L52L29, 1953.

6. Cahn, Maurice S.: An Experimental Investigation of Sting-Support Effects on Drag and a Comparison With Jet Effects at Transonic Speeds. NACA Rep. 1353, 1958. (Supersedes NACA RM L56F18a.)

7. Hall, Charles F.: Lift, Drag, and Pitching Moment of Low-Aspect-Ratio Wings at Subsonic and Supersonic Speeds. NACA RM A53A30, 1953.

8. Flax, A. H., and Lawrence, H. R.: The Aerodynamics of Low-Aspect-Ratio Wings and Wing-Body Combinations. Rep. No. CAL-37, Cornell Aero. Lab., Inc., Sept. 1951.

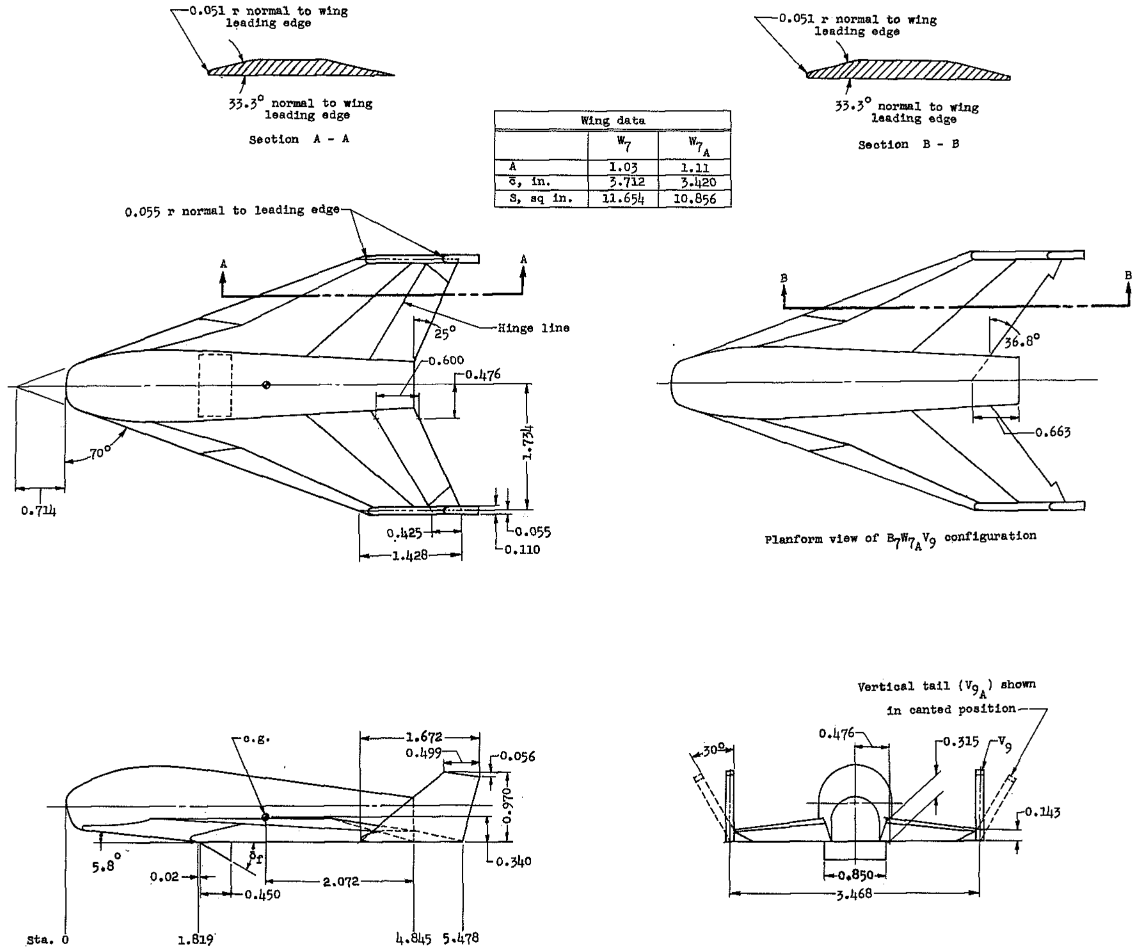

Wing data		
	W_7	W_{7_A}
A	1.03	1.11
$\bar{c}$, in.	3.712	3.420
S, sq in.	11.654	10.856

Figure 1.- Model sketches and design dimensions for configuration $B_7F_4W_7V_9$ and also for configuration $B_7W_{7_A}V_9$ and vertical tail V_{9_A} where indicated. All dimensions are in inches unless otherwise noted.

[redacted]

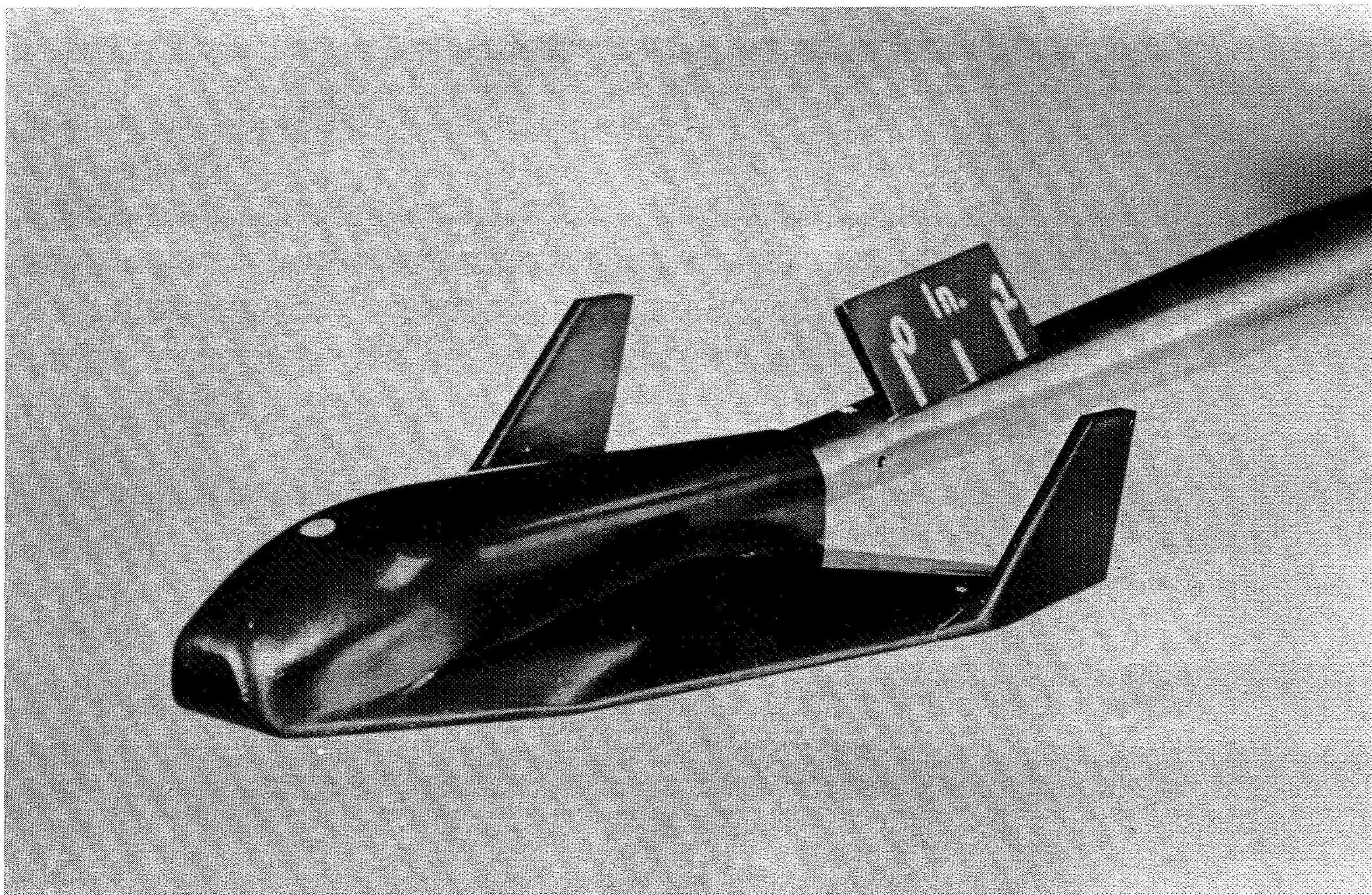

Figure 2.- Photograph of model $B_7W_7V_9$. L-59-1724

[redacted]

[redacted]

L-745

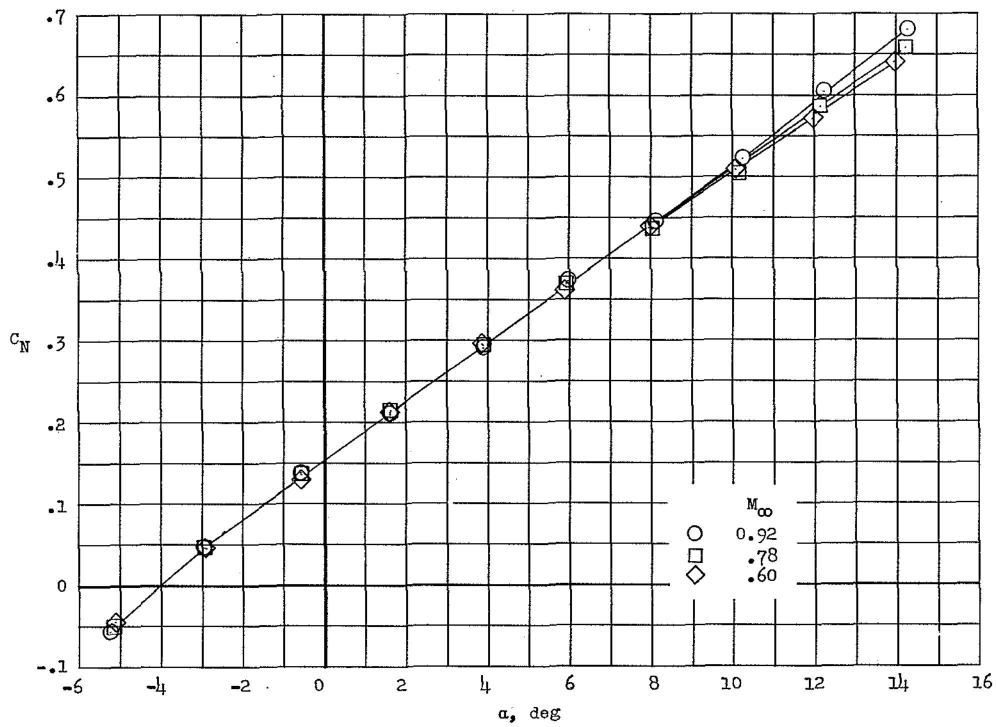

(a) C_N against α.

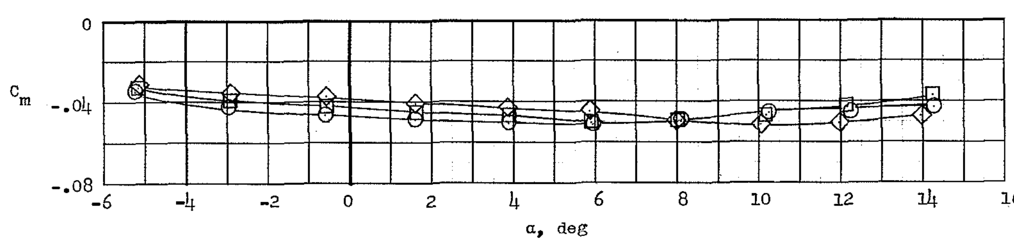

(b) C_m against α.

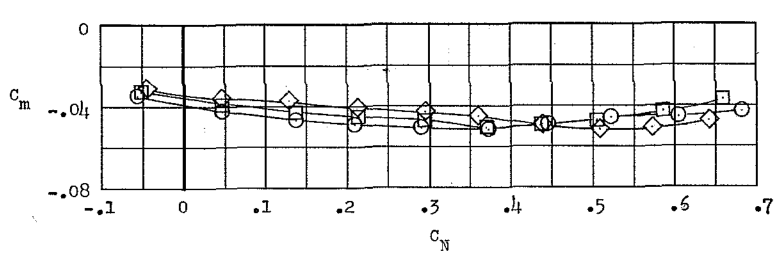

(c) C_m against C_N.

Figure 3.- Effect of Mach number on the longitudinal aerodynamic characteristics of model $B_7W_7V_9$. $\beta = -0.2^\circ$.

[redacted]

L-745

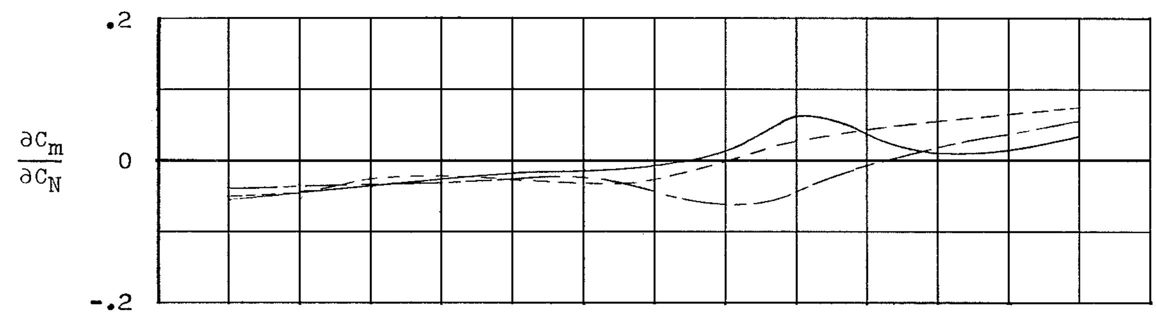

(a) Longitudinal stability parameter.

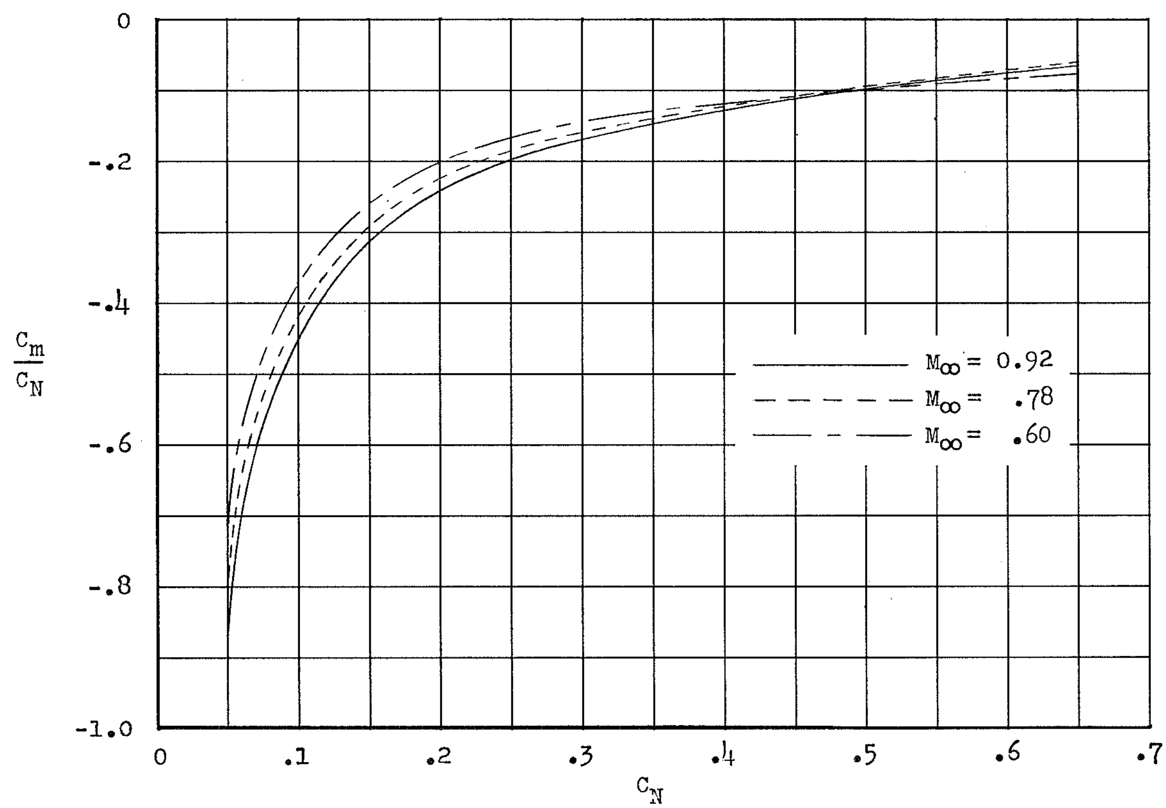

(b) Longitudinal center of pressure.

Figure 4.- Effect of Mach number on the longitudinal stability parameter and longitudinal center-of-pressure location for model $B_7W_7V_9$.

[redacted]

[redacted]

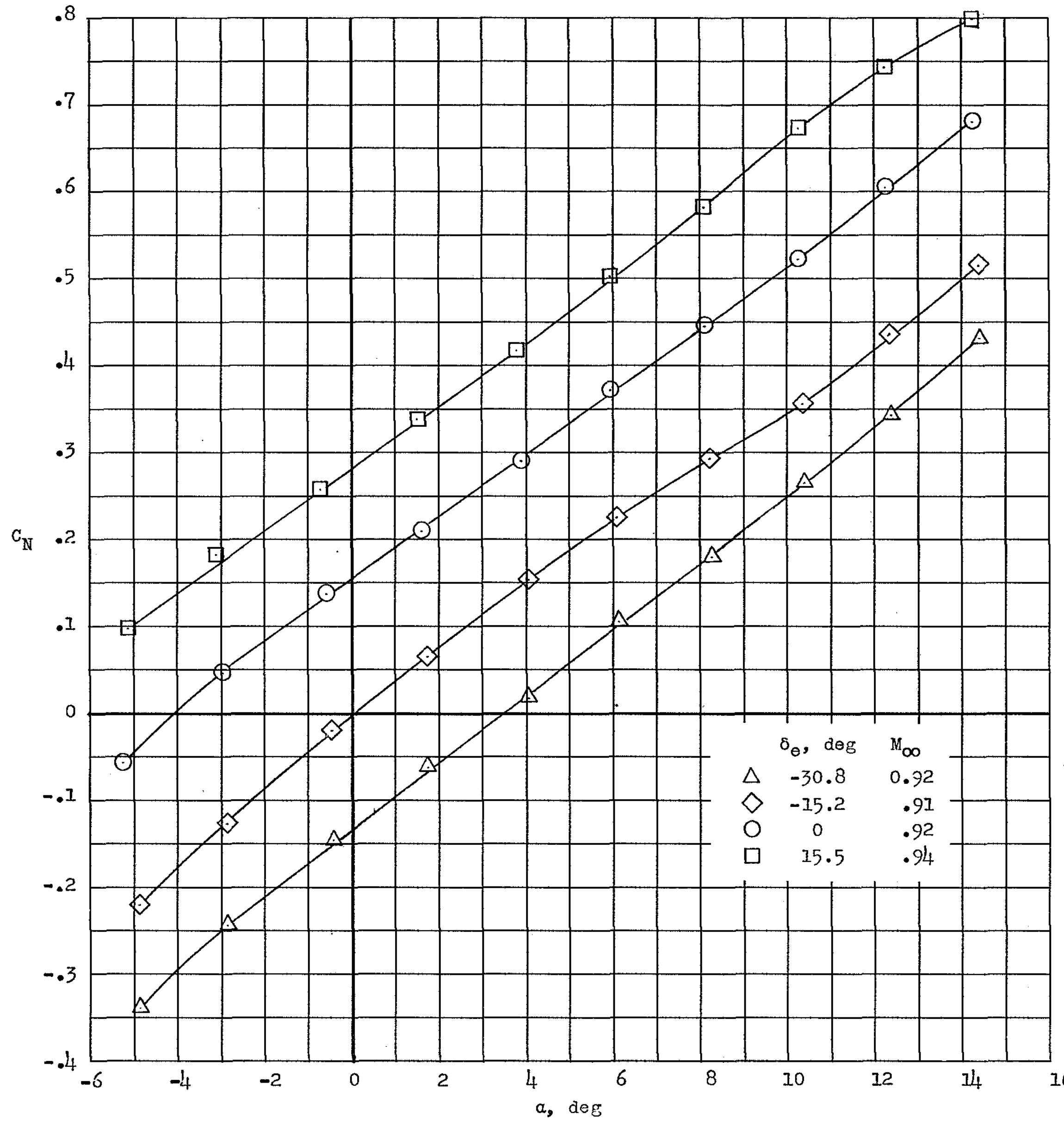

(a) C_N against α.

Figure 5.- Effect of elevon deflection on the longitudinal aerodynamic characteristics of model $B_7W_7V_9$. $\beta = -0.2^{\circ}$.

L-745

[redacted]

L-745

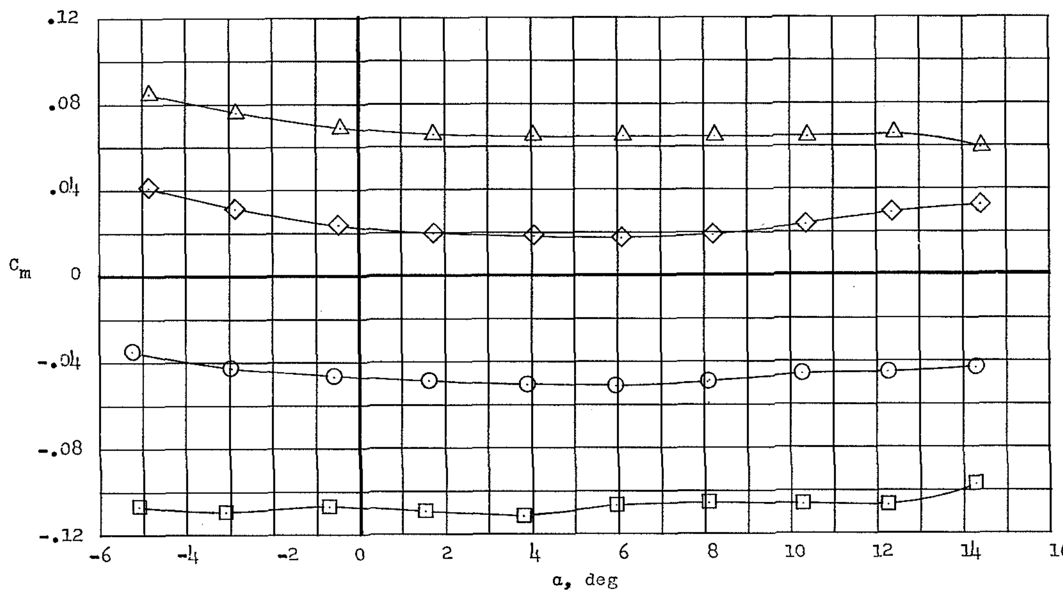

(b) C_m against α.

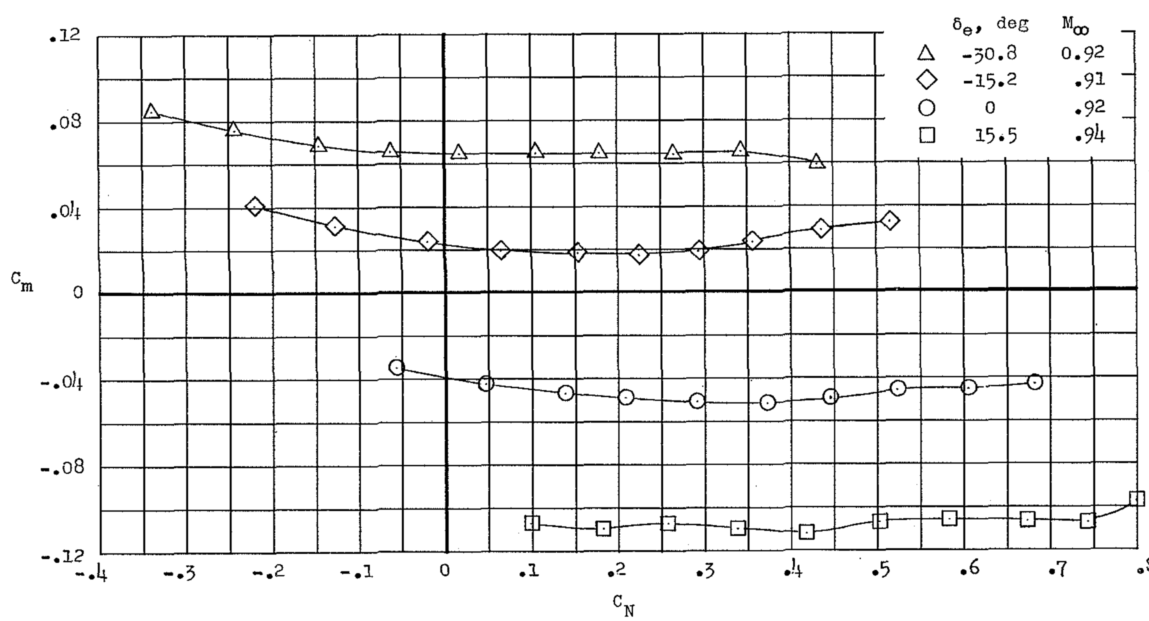

(c) C_m against C_N.

Figure 5.- Concluded.

[redacted]

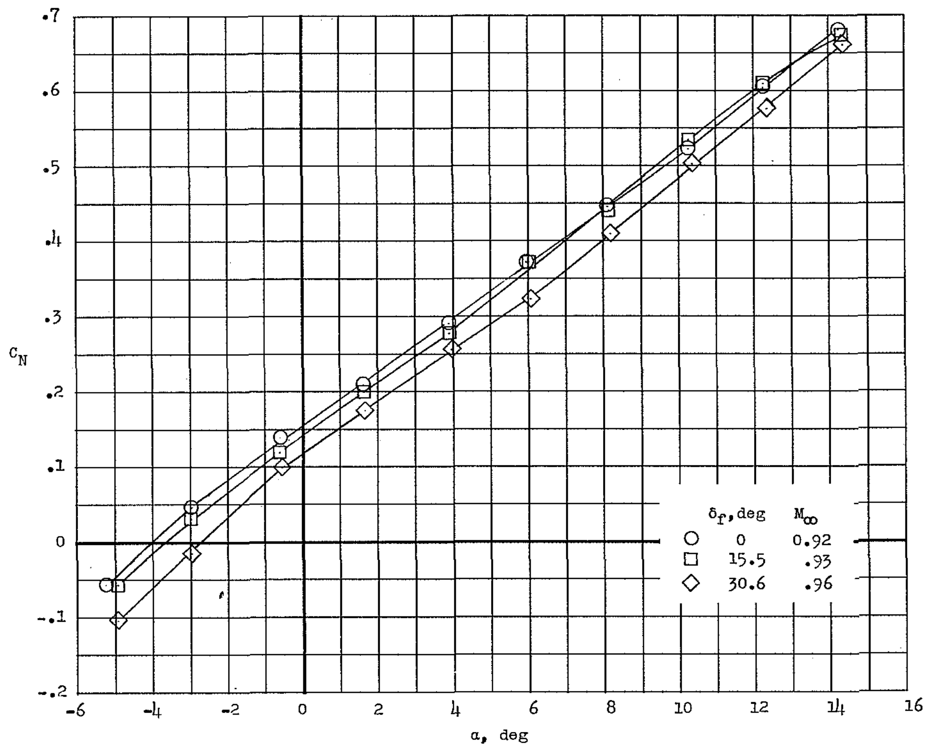

(a) C_N against α.

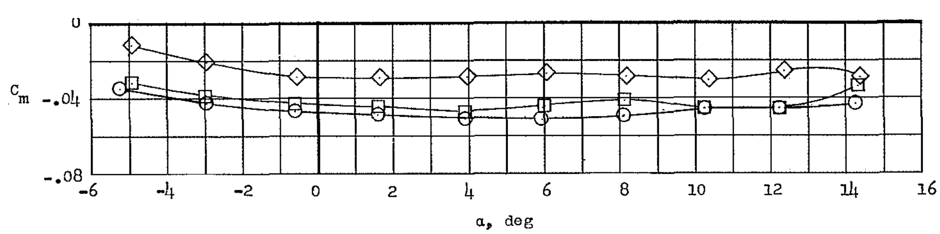

(b) C_m against α.

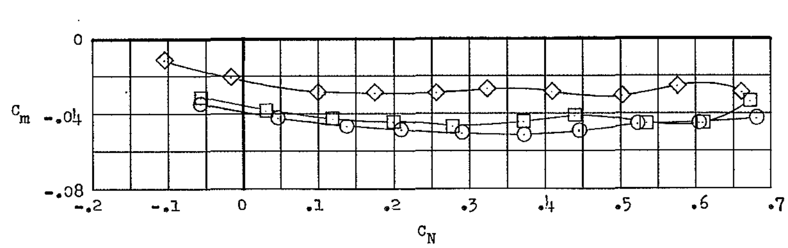

(c) C_m against C_N.

Figure 6.- Effect of body flap F_4 deflection on the longitudinal aerodynamic characteristics of model $B_7W_7V_9$. $\beta = -0.2^{\circ}$.

L-745

[redacted]

L-745

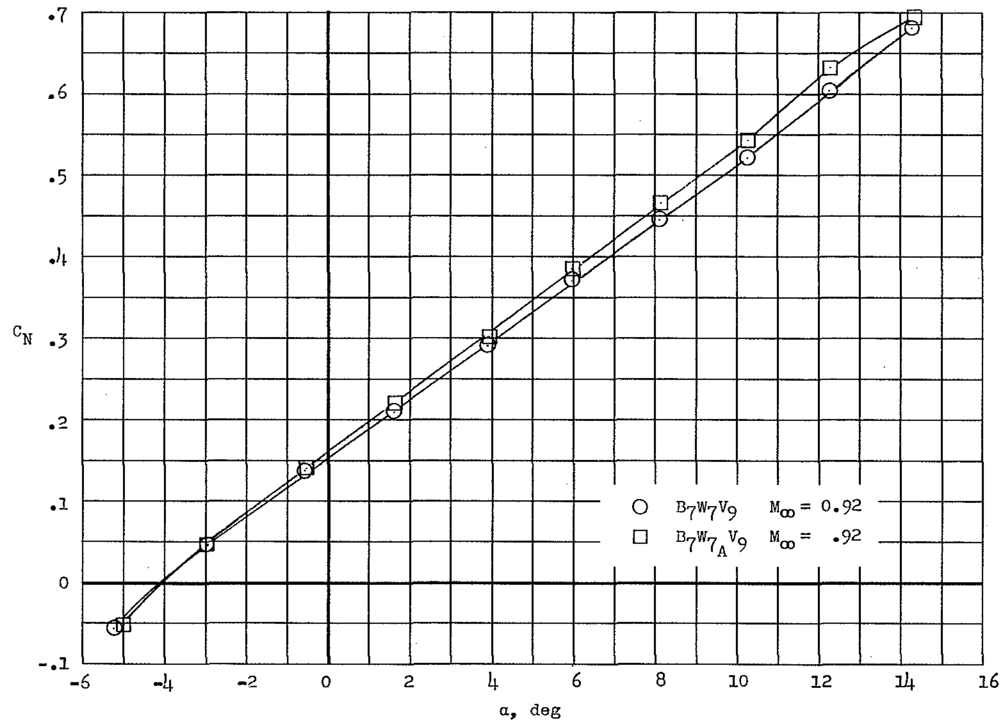

(a) C_N against α.

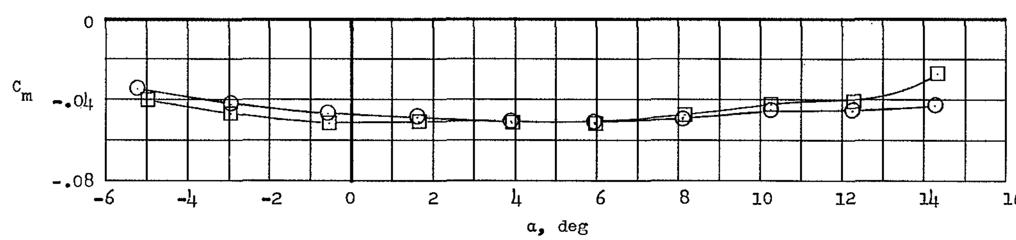

(b) C_m against α.

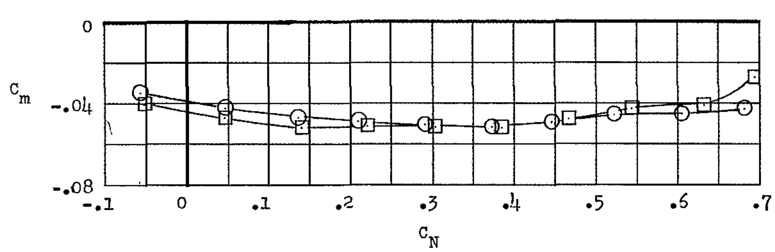

(c) C_m against C_N.

Figure 7.- Comparison of longitudinal aerodynamic characteristics for models $B_7W_7V_9$ and $B_7W_{7_A}V_9$. $\beta = -0.2^\circ$.

[redacted]

[redacted]

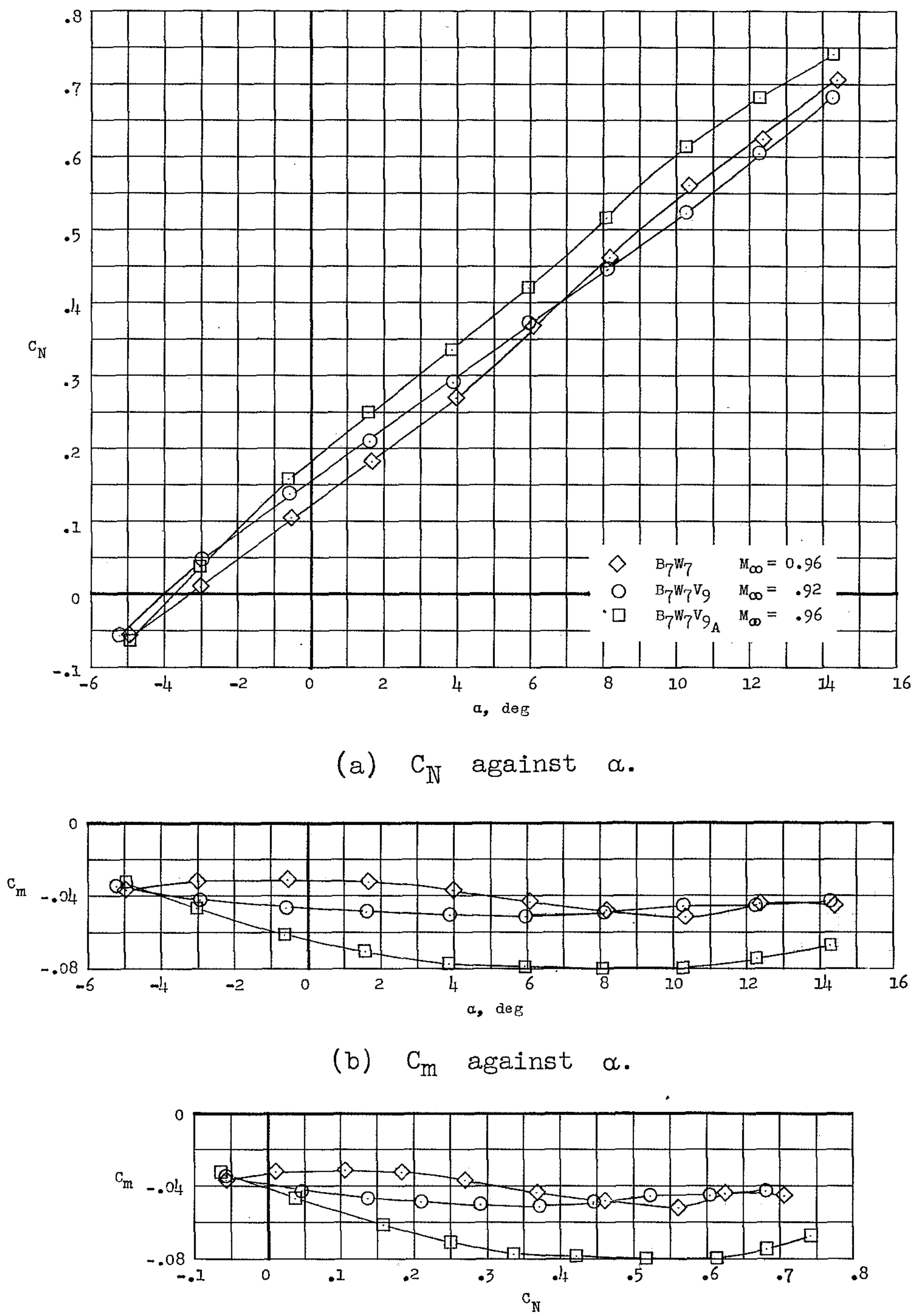

(a) C_N against α.

(b) C_m against α.

(c) C_m against C_N.

Figure 8.- Effect of tail configuration on the longitudinal aerodynamic characteristics of model B_7W_7. $\beta = 0.2^\circ$.

[redacted]

L-745

L-745

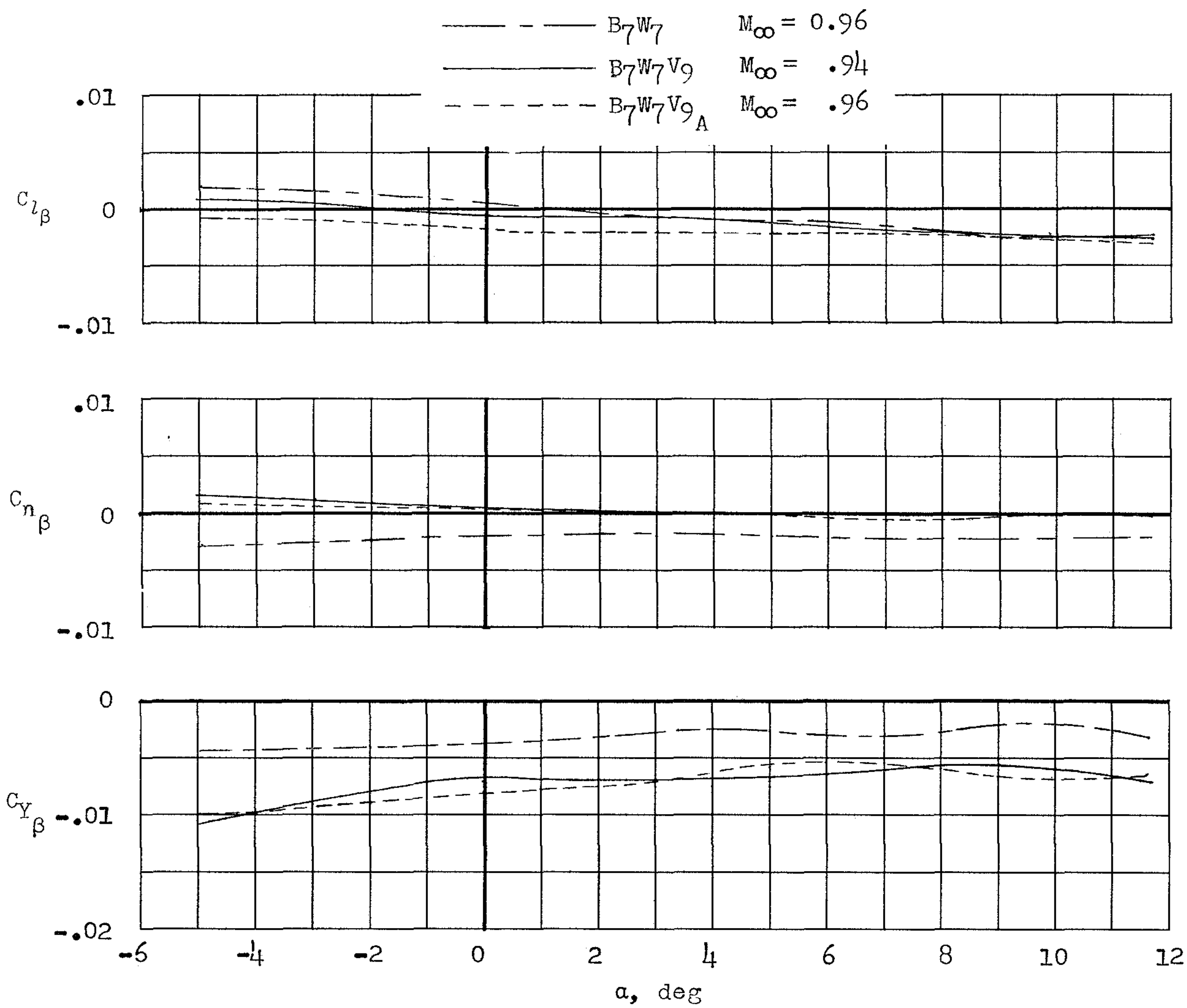

Figure 9.- Effect of tail configuration on the lateral stability derivatives of model B_7W_7.

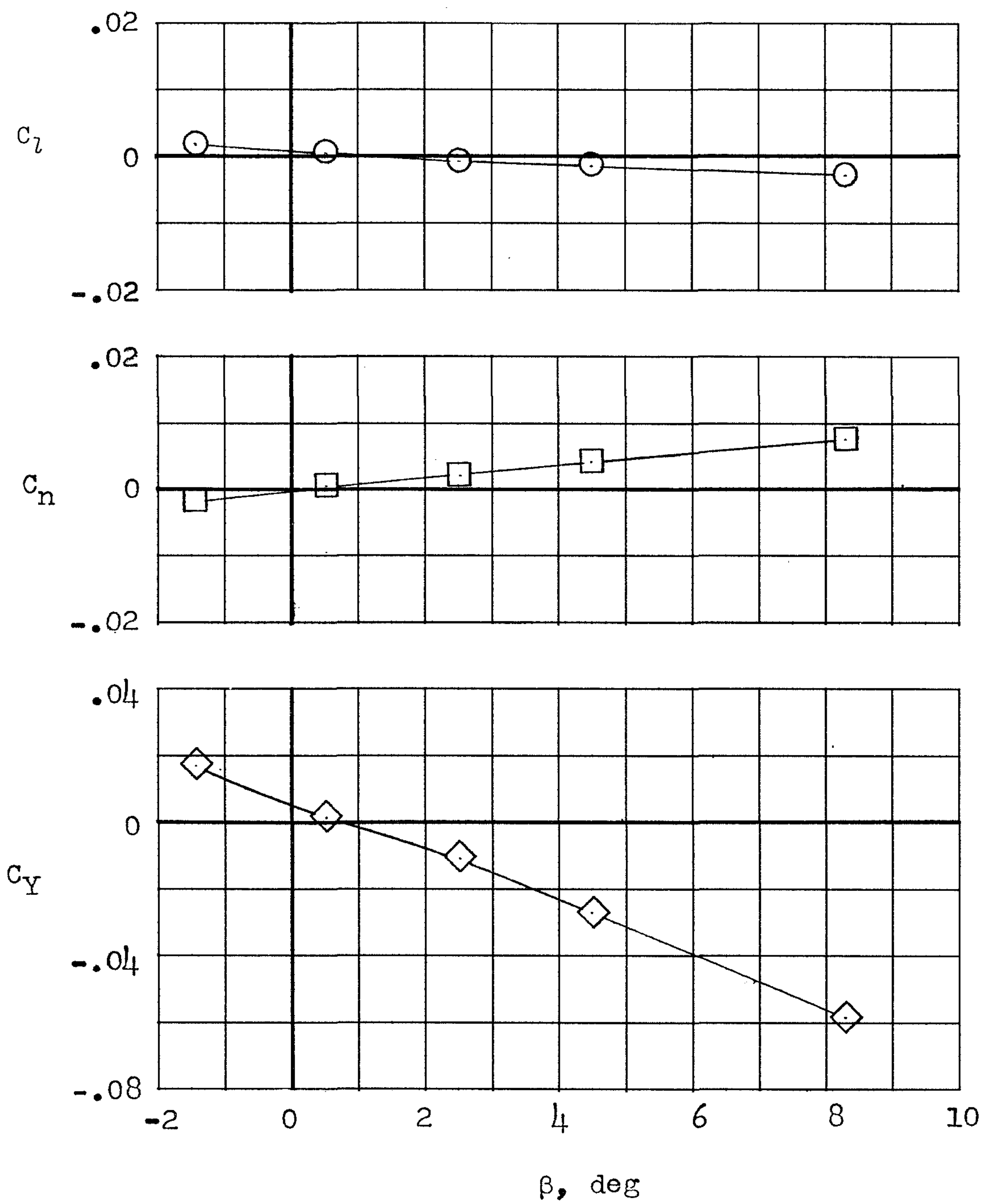

Figure 10.- Effect of sideslip angle on C_l, C_n, and C_Y for model $B_7W_7V_9$. $\alpha = 0^{\circ}$; $M_\infty = 0.94$.

L-745

[redacted]